Electron Donor–Acceptor Interactions in Regioselectively Synthesized exTTF2–C70(CF3)10 Dyads

ARTICLE *in* CHEMISTRY - A EUROPEAN JOURNAL · MARCH 2010

Impact Factor: 5.73 · DOI: 10.1002/chem.200902336 · Source: PubMed

10 AUTHORS, INCLUDING:

Gustavo de Miguel Rojas
University of Cordoba (Spain)
34 PUBLICATIONS **572** CITATIONS
SEE PROFILE

Ivan E Kareev
Russian Academy of Sciences
33 PUBLICATIONS **739** CITATIONS
SEE PROFILE

Olga V. Boltalina
Colorado State University
268 PUBLICATIONS **4,242** CITATIONS
SEE PROFILE

Takahiro Tsuchiya
Kitasato University
122 PUBLICATIONS **3,909** CITATIONS
SEE PROFILE

DOI: 10.1002/chem.200902336

Electron Donor–Acceptor Interactions in Regioselectively Synthesized exTTF$_2$–C$_{70}$(CF$_3$)$_{10}$ Dyads

Yuta Takano,[a, b] M. Ángeles Herranz,[a] Nazario Martín,*[a] Gustavo de Miguel Rojas,[c] Dirk M. Guldi,*[c] Ivan E. Kareev,[d] Steven H. Strauss,*[e] Olga V. Boltalina,*[e] Takahiro Tsuchiya,[b] and Takeshi Akasaka*[b]

Dedicated to Professor Josep M. Ribó on the occasion of his 70th birthday

Abstract: The decakis(trifluoromethyl)fullerene C_1-C$_{70}$(CF$_3$)$_{10}$, in which the CF$_3$ groups are arranged on a *para*[7]*-meta-para* ribbon of C$_6$(CF$_3$)$_2$ edge-sharing hexagons, and which has now been prepared in quantities of hundreds of milligrams, was reacted under standard Bingel–Hirsch conditions with a bis-π-extended tetrathiafulvalene (exTTF) malonate derivative to afford a single exTTF$_2$–C$_{70}$(CF$_3$)$_{10}$ regioisomer in 80% yield based on consumed starting material. The highly soluble hybrid was thoroughly characterized by using 1D ^{1}H, ^{13}C, and ^{19}F NMR, 2D NMR, and UV/Vis spectroscopy; matrix-assisted laser desorption ionization (MALDI) mass spectrometry; and electrochemistry. The cyclic voltammogram of the exTTF$_2$–C$_{70}$(CF$_3$)$_{10}$ dyad revealed an irreversible second reduction process, which is indicative of a typical retro-Bingel reaction; whereas the usual phenomenon of exTTF inverted potentials ($E^1_{ox} > E^2_{ox}$), resulting in a single, two-electron oxidation process, was also observed. Steady-state and time-resolved photolytic techniques demonstrated that the C_1-C$_{70}$(CF$_3$)$_{10}$ singlet excited state is subject to a rapid electron-transfer quenching. The resulting charge-separated states were identified by transient absorption spectroscopy, and radical pair lifetimes of the order of 300 ps in toluene were determined. The exTTF$_2$–C$_{70}$(CF$_3$)$_{10}$ dyad represents the first example of exploitation of the highly soluble trifluoromethylated fullerenes for the construction of systems able to mimic the photosynthetic process, and is therefore of interest in the search for new materials for photovoltaic applications.

Keywords: donor–acceptor systems · electrochemistry · electron transfer · fullerenes · tetrathiafulvalene · trifluoromethylated fullerenes

[a] Y. Takano, Dr. M. Á. Herranz, Prof. Dr. N. Martín
Departamento de Química Orgánica I
Facultad de Química, Universidad Complutense
28040 Madrid (Spain)
Fax: (+34) 91-394-4103
E-mail: nazmar@quim.ucm.es

[b] Y. Takano, Dr. T. Tsuchiya, Prof. Dr. T. Akasaka
Center for Tsukuba Advanced Research Alliance
University of Tsukuba
305-8577 Ibaraki (Japan)
Fax: (+81) 298-53-6409
E-mail: akasaka@tara.tsukuba.ac.jp

[c] Dr. G. de Miguel Rojas, Prof. Dr. D. M. Guldi
Friedrich-Alexander-Universität Erlangen-Nürnberg
Department of Chemistry and Pharmacy &
Interdisciplinary Center for Molecular Materials (ICMM)
Egerlandstrasse 3, 91058 Erlangen (Germany)
Fax: (+49) 9131-852-8307
E-mail: dirk.guldi@chemie.uni-erlangen.de

[d] Dr. I. E. Kareev
Institute of Problems of Chemical Physics
Russian Academy of Sciences
Chernogolovka 142432 (Russia)

[e] Prof. Dr. S. H. Strauss, Dr. O. V. Boltalina
Department of Chemistry, Colorado State University
Fort Collins, Colorado 80523 (USA)
Fax: (+1) 970-491-1801
E-mail: steven.strauss@colostate.edu
olga.boltalina@colostate.edu

Supporting information for this article is available on the WWW under http://dx.doi.org/10.1002/chem.200902336.

Introduction

Several sophisticated and versatile synthetic strategies have been pursued in recent years in order to prepare donor–acceptor dyads capable of undergoing photoinduced energy or electron transfer in artificial photosynthetic and photovoltaic model systems.[1,2] Fullerenes, in particular [60]fullerene, present outstanding physicochemical properties in a three-dimensional structure (accepting up to six electrons in solution at moderate reduction potentials to form stable anionic species and, simultaneously, exhibiting very low reorganization energies in charge transfer reactions), which render them attractive candidates for energy conversion and energy storage.[3,4] In addition, *p*-quinonoid π-extended tetrathiafulvalenes (exTTFs) are exceptional materials for molecular-scale electronic applications. Unlike many known electron donors, exTTF undergoes aromatization upon oxidation and affords a thermodynamically stable dicationic species at relatively low oxidation potentials.[5] Moreover, the formation of aromatic species upon oxidation is accompanied by a dramatic geometrical change, from a butterfly-shaped neutral state to a planar dicationic structure, which additionally stabilizes the charged species.[5] The covalent linking of the electron donor, exTTF, with the electron acceptor, C_{60}, has allowed the preparation of a plethora of photo- and electroactive dyads able to act as artificial photosynthetic systems and active molecular materials in organic photovoltaics.[6]

The ability of carbon to exist in different allotropic forms has provided, in addition to C_{60}, new varieties of nanoscale shapes with fascinating properties. These include higher fullerenes, endohedral fullerenes, and single- and multi-walled carbon nanotubes.[7] A singular and less-known family of carbon nanostructures with pronounced acceptor properties is the fluorinated fullerenes.[8] Their good solubility, high reactivity towards nucleophiles, and enhanced dienophilicity of the remainder of the fullerene system, together with their significantly enhanced electron affinities, offer an improved alternative to bare fullerenes or organofullerenes as synthons for the synthesis of donor–acceptor complexes. However, most of the known fluorination reactions yield products with high addition degree, for example, in the case of $C_{60}F_x$, compounds with $x = 36$–46 are typically produced.[9] Only two such products, $C_{60}F_{36}$ and $C_{60}F_{48}$, can be made in synthetically useful quantities and with high yields.[10] However, chemical modifications of these compounds are difficult to perform, because of the lack of sterically accessible sites for the addition of bulky groups and because of the potentially large number of substitution products. The only fluorofullerene with a lower number of F atoms which can be selectively prepared in large quantities is $C_{60}F_{18}$,[11] for which some chemical transformations have been performed[12] and the photophysical properties of donor–acceptor complexes have been studied.[13]

More recently, we have developed efficient synthetic methodologies and isolation procedures for a different class of fluorine-containing fullerenes, the perfluoroalkylfullerenes (PFAFs).[14] Unlike fluorofullerenes, PFAFs exhibit reversible redox behavior as well as superior solubility and thermal stability.[15] PFAFs can be prepared in a wide range of compositions, including compounds with just two or four R_f groups, and in some cases with high selectivity. In particular, trifluoromethylation of C_{70} resulted in the isolation of one isomer of a particular composition, C_1-$C_{70}(CF_3)_{10}$, in 60% yield based on converted C_{70}.[11,15b,16] In this isomer, there are two remaining $C(sp^2)_5$ pentagons. All four isomers of $C_{70}(CF_3)_{12}$ have the C_1-$C_{70}(CF_3)_{10}$ addition pattern plus two additional CF_3 groups, which have been added to one or both of those pentagons.[15b] As discussed below, the [6,6] double bond connecting the $C(sp^2)_5$ pentagons in C_1-$C_{70}(CF_3)_{10}$ should be the most reactive bond for cycloadditions.

Herein, we report the high-yield preparation and characterization of a dyad composed of the C_1-$C_{70}(CF_3)_{10}$ acceptor moiety and an exTTF electron-donor moiety. The dyad is a cycloadduct of C_1-$C_{70}(CF_3)_{10}$, and, as anticipated, it was obtained primarily as a single isomer. It has been fully characterized by spectroscopic and electrochemical techniques, and studied in detail by photophysical methods. This is the first donor–acceptor dyad that includes a fullerene$(CF_3)_n$ acceptor moiety. In addition, we have demonstrated for the first time that the preparation of C_1-$C_{70}(CF_3)_{10}$ can be scaled up to afford hundreds of milligrams of pure compound, making it an attractive synthon for future photophysical studies and potential practical applications.

Results and Discussion

Synthesis and spectroscopic characterization: Advances in fullerene applications are often hampered by the limited availability of starting materials, especially derivatized fullerenes. Therefore, in this work we made an effort to improve the yield and efficiency for the synthesis of C_1-$C_{70}(CF_3)_{10}$ (**1**). Our previous report on the 60% yield of this compound involved the use of 30 mg of C_{70} and CF_3I gas in a heated flow tube with a reaction time of 1.5 h.[15b] Among the reported preparative methods for fullerene$(CF_3)_n$ derivatives,[14,17] the heated-flow-tube method is attractive because it affords high selectivity and high conversion and combines short reaction times, technical simplicity, and easy scalability. For comparison, the yield of **1** from 42 mg of C_{70} and CF_3I in a sealed tube at 400 °C was only 32%, and it required a reaction time of 110 h.[17]

Table 1 lists reaction conditions and yields of $C_{70}(CF_3)_n$ products obtained in reactions in the heated flow tube. These data demonstrate that increasing the amount of C_{70} from 30 to 200 mg did not result in a decrease in the yield or conversion percentages. Furthermore, the addition of Cu powder to these reactions led to significantly higher reaction rates, which allowed us to keep the reaction times to 1–2 h despite the larger scale, thereby using CF_3I gas more efficiently. A straightforward two-stage HPLC separation procedure (1: toluene; 2: 20/80 v/v toluene/heptane) was performed on the combined crude products from reactions 1, 3, and 4 listed in Table 1, and this resulted in the isolation of

Table 1. Experimental data on the synthesis of **1** from C_{70} and CF_3I in the heated flow tube.

Experiment	Mass of C_{70} [mg]	Mass of Cu [mg]	T [°C]	t [min]	Mass of $C_{70}(CF_3)_x$ [mg]	x in $C_{70}(CF_3)_x$	Yield [mol %]
1	98	200	520	60	123	8, 10	72
2	210	300	520	120	288	8, 10	79
3	214	200	520	150	280	8, 10	75
4	206	450	550	150	256	8, 10	71

0.48 g of **1** that was 98 mol % pure. A portion of this amount was used for the chemical derivatizations of **1** performed in this work, which are depicted in Figure 1.

The fact that **1** has an asymmetric addition pattern consisting of a ribbon of nine edge-sharing *meta*- and/or *para*-$C_6(CF_3)_2$ hexagons was first revealed by ^{19}F NMR spectroscopy.[14c] X-ray crystallography later revealed the unprecedented *para*^{7}-*meta*-*para* addition pattern.[16] A thermal-ellipsoid plot of **1** is shown in Figure 1, along with a partially numbered Schlegel diagram, and a pyracyclene-like fullerene fragment. There are only eight remaining [6,6] double bonds in **1** that are part of pyracyclene fragments (i.e., double bonds that are common to $C(sp^2)_6$ hexagons), but only one of them, C33=C34, is part of a pyracyclene fragment that also includes two $C(sp^2)_5$ pentagons. The C33=C34 bond is also the only one of the eight for which both C atoms have pyramidalization (POAV) angles greater than 11.0° (C33 and C34 both have POAV angles of 11.9°).[16] This bond is therefore the most accessible sterically as well as one of the most reactive double bonds in **1**, and consequently it is the expected site for cycloaddition.

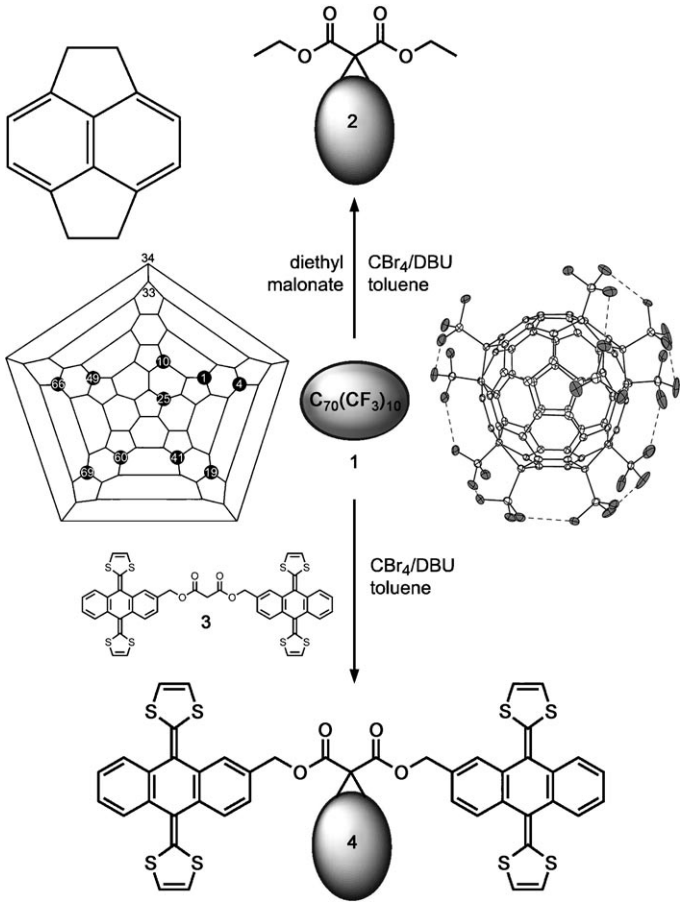

Figure 1. The transformations of **1** into Bingel–Hirsch cycloadducts **2** and **4**. Also shown are the X-ray structure and IUPAC-numbered Schlegel diagram of **1**, and a pyracyclene-like fullerene fragment showing a [6,6] double bond in the center (such as the reactive bond C33=C34 in **1**).

With these considerations in mind, we decided to explore the reactivity of **1** under Bingel–Hirsch conditions,[18] reacting it with diethyl malonate in the presence of CBr_4 and diazabicyclo[4.2.0]undec-7-ene (DBU), as shown in Figure 1. The reaction progressed very rapidly at room temperature, and after one hour the formation of the expected Bingel derivative **2** was complete. Purification by flash chromatography using a hexane/CH_2Cl_2 mixture followed by a one-step HPLC separation (see Figure S1 in the Supporting Information) resulted in the isolation of **2** in 48 % yield. The MALDI-TOF mass spectrum of **2** was obtained using tetracyano-*p*-quinodimethane (TCNQ) as the matrix, and showed not only the molecular-ion isotope pattern, but also the ion with the isotope pattern corresponding to the loss of one CF_3 group (see Figure S2 in the Supporting Information). This fragmentation is typical of fullerene$(CF_3)_n$ compounds, and was observed for both derivatives reported in this work. While this work was in progress, the synthesis and X-ray structure of **2** was reported by another group.[17] This group also reported DFT calculations that predicted the high reactivity of the C33=C34 bond.[17]

Following the successful preparation of **2**, the synthesis of an electroactive dyad was accomplished by the reaction of **1** with di[9,10-bis(1,3-dithiol-2-ylidine)-9,10-dihydro-2-anthracenylhydroxymethyl] malonate (**3**)[19] in the presence of CBr_4 and DBU, as also shown in Figure 1. The reaction proceeded smoothly as in the synthesis of **2**, and, after flash column chromatography and a one-step HPLC separation, the very pure monoadduct **4** was obtained in 80 % yield based on consumed C_1-$C_{70}(CF_3)_{10}$, as shown in Figure 2.

Compound **4** was fully characterized by spectroscopic and electrochemical methods, and its MALDI-TOF mass spectrum, shown in Figure 3, confirmed its composition. The most prominent group of peaks in the spectrum, the most intense of which is 2416.95 m/z (calcd. 2416.92 m/z), corresponds to the $[C_{70}(CF_3)_{10}\{C(CO_2CH_2exTTF)_2\}]^+$ molecular ion; a fragment ion due to the loss of one CF_3OH group was also observed at 2330.99 m/z. The electronic absorption spectrum of **4**, shown in Figure 4, revealed the characteristics of its two components, C_1-$C_{70}(CF_3)_{10}$ and exTTF **3**. Note that the intermolecular interaction of **4** was not observed in the range between 5.00×10^{-6} M and 6.00×10^{-4} M in $CHCl_3$.

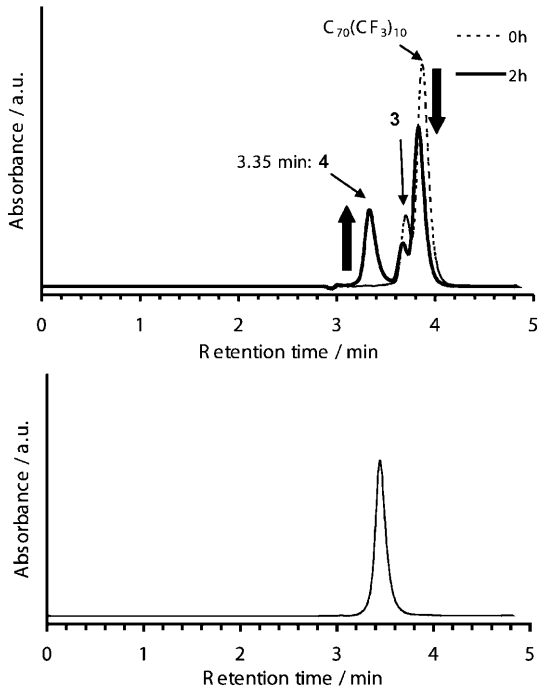

Figure 2. HPLC profiles of the reaction mixture (top) and the purified product (bottom) in the synthesis of **4** (4.6×250 mm Buckyprep column; eluent 10:90 v/v methanol/toluene; flow rate 1.0 mL min^{-1}; room temperature; detector wavelength 330 nm).

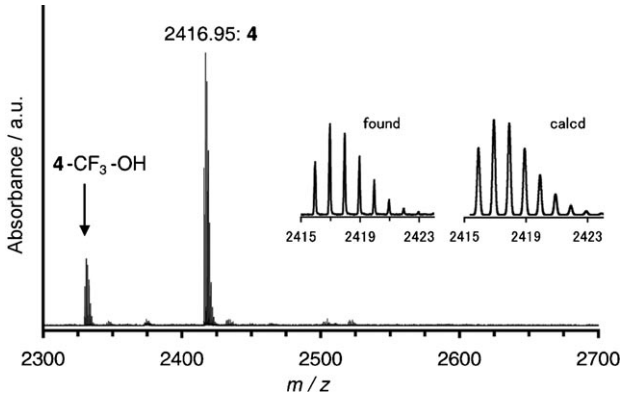

Figure 3. MALDI-TOF mass spectrum of **4**. Dithranol was used as the matrix.

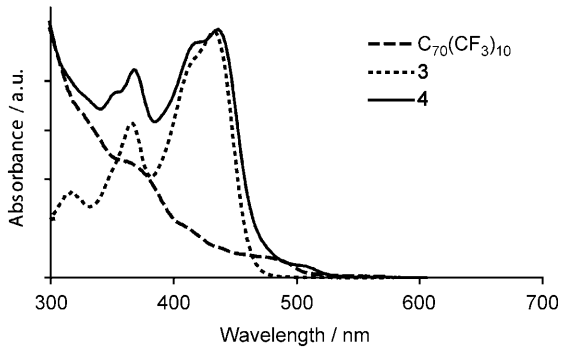

Figure 4. UV/Vis spectra of C_1-$C_{70}(CF_3)_{10}$, **3**, and **4** in $CHCl_3$.

The MALDI-TOF mass spectrum of **4** did not show the formation of dimers or oligomers by aggregation.

^{1}H and ^{13}C NMR spectra of **4** showed the presence of a single regioisomer (see Figures S3 and S4, respectively, in the Supporting Information). The ^{1}H NMR spectrum clearly showed the spectral pattern of the exTTF groups. The resonances for the aromatic protons of the anthracenyl group are between $\delta = 7.77$ and 7.41 ppm, and between $\delta = 7.26$ and 6.93 ppm; the multiplets at $\delta \approx 6.4$ ppm correspond to the protons of the 1,3-dithiole rings; and the signals between $\delta = 5.42$ and 5.15 ppm are assigned to the AB quartet of the diastereotopic geminal protons in the methylene groups. The ^{13}C NMR spectrum showed a total of 103 lines (of 125 carbon signals), which indicates that **4** has the expected C_1 symmetry. The ten quartets between $\delta = 62.3$ and 57.3 ppm are assigned to the cage C(sp^3) atoms bonded to the CF_3 groups (see Figure S5 in the Supporting Information), and the quartets between $\delta = 122.8$ and 122.2 ppm are assigned to the ten CF_3 carbon atoms (see Figure S6 in the Supporting Information). The J_{FC} values for the C(sp^3) atoms have ranges of 32.1–34.5 and 280.0–282.5 Hz, respectively. The signals at $\delta = 70.9$ and 69.1 ppm are assigned to the cage C-(sp^3) atoms that are part of the exocyclic cyclopropane ring, and the signal at $\delta = 43.9$ ppm is assigned to the third C(sp^3) atom of the cyclopropane ring. The signals for the methylene carbon atoms were observed at $\delta = 68.4$ and 68.3 ppm. Full assignment of all resonances signals was accomplished using DEPT135, HMQC, and HMBC techniques (see Figures S7–S9 in the Supporting Information).

The ^{19}F NMR spectra of **1** and **4**, shown in Figure 5, exhibit through-space Fermi-contact $^{6,7}J_{FF}$ coupling through direct overlap of fluorine lone-pair orbitals.[20] This is common for fullerene(CF_3)$_n$ derivatives, and has been discussed in the previous work of some of us. The chemical shifts and coupling constants for **1** and **4**, listed in Table 2, are very similar (the 1D and 2D ^{19}F NMR spectra of **1** have been reported previously;[14c] the 1D spectrum is included here for comparison with the spectrum of **4**). Also shown in Figure 5 is the ^{19}F NMR spectrum of the 3,6-dimethoxy *o*-quinodimethane cycloadduct of $C_{70}(CF_3)_{10}$ (i.e., $C_{70}(CF_3)_{10}$(3,6-DMQDM), **5**), the synthesis and X-ray structure of which we reported recently.[21] Note that the multiplets for **5** are all shielded relative to the corresponding multiplets for **1**. Two multiplets in particular, **a** and **d**, are shielded the most and broadened the most, due to the equilibration of the two possible boat conformations of the exocyclic six-membered ring. In contrast, the multiplets of **4** are both shielded (multiplets **a**, **c**, **e**, and **i**) and deshielded (multiplets **d** and **g**).

Two views of the structure of **5** and a portion of one possible conformation of **4**, based on the X-ray structure of **2**[17] (with two exTTF groups replacing two CH_3 groups), are shown in Figure 6. It is clear that as the aromatic ring in **5** is flipped from one side of the fullerene to the other, the CF_3 groups on C4 and C66 (which are assigned to multiplets **a** and **d**, respectively) will experience the greatest shielding, and the CF_3 groups on C1, C19, C49, and C69 (multiplets **c**, **g**, **i**, and **e**) will experience the next greatest shielding. It is

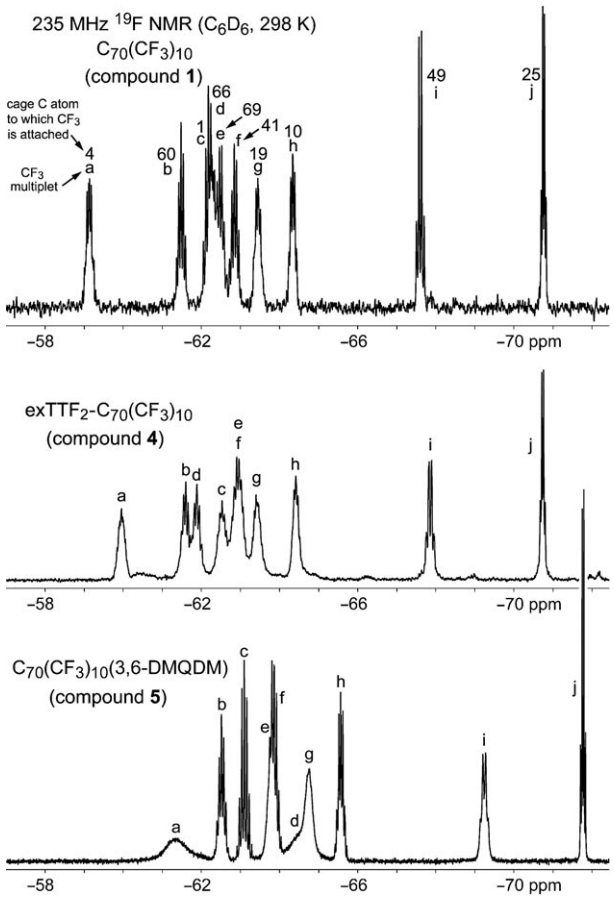

Figure 5. NMR spectra of **1** (top), **4** (middle), and **5** (bottom) in C_6D_6 at 235.4 MHz.

also clear that the Bingel ester moieties in **4** can exhibit a much wider range of conformations than the six-membered ring in **5**, and they can presumably have time-averaged conformations that put the six closest CF_3 groups in either the shielding or deshielding regions of the exTTF aromatic rings. The multitude of conformations leads to: 1) smaller multiplet shifts for **4** than for **5** relative to the corresponding δ values for **1**, and 2) shifts that are due to both net shielding and net deshielding, depending on the position of the CF_3 group.

Electrochemistry: The electrochemical behavior of compounds **1**–**4** has been investigated by cyclic voltammetry (CV) and differential pulse voltammetry (DPV) in THF, as shown in Figure 7 and Table 3. Compound **1** exhibits three fullerene-based reductions. The first reduction at $E^1_{red} = -0.947$ V is electrochemically irreversible, although chemically reversible, since the reduction current recorded for multiple cycles remained the same.[15b] This is followed by a second reversible reduction ($E^2_{red} = -1.528$ V) and a third irreversible process ($E^3_{red} = -2.213$ V). It is known that upon fullerene mono-cycloaddition, loss of conjugation leads to a LUMO that is higher in energy and thus to a decreased electron affinity for derivatized fullerenes.[22] For this reason, the reduction potentials of the Bingel derivatives **2** and **4** are shifted towards more negative values ($\approx$100 mV for the first reduction process). Methanofullerene **2** exhibits two reversible fullerene-based reductions at $E^1_{red} = -1.102$ V and $E^2_{red} = -1.696$ V. The third reduction at $E^3_{red} = -1.822$ V is chemically irreversible, presumably due to the cleavage of one of the cyclopropane bonds connecting the addend to **1**.[23]

The C_{70}-Bingel dyad **4** shows electrochemical reversibility only for the first reduction step ($E^1_{red} = -1.154$ V) on the cyclic voltammetric timescale at 100 mV s^{-1}. The voltammogram turned out to be irreversible at the second reduction potential, at which a retro-cyclopropanation reaction probably occurs.[24] On the oxidation side, the two-electron quasi-reversible oxidation, forming the exTTF dication directly, is observed at $E^1_{ox} = +0.07$ V.[25]

Similar redox potentials, as found for **3** and **2**, reveal, in agreement with the data stemming from the electronic spectra, only weak interactions between the redox chromophores in their ground state.

Photophysics: To study the electronic interactions between C_1-$C_{70}(CF_3)_{10}$ and exTTF in the excited state, emission measurements were carried out with **4** in solvents of different polarity (i.e., toluene, THF, and benzonitrile). The data are always set in relation to **1** and **2**, which lack the electron-donating exTTF. As Figure 8 demonstrates, **1** and **2** fluoresce with similar quantum yields, that is, 0.018 and 0.025, respectively. In sharp contrast, attaching the electron-donating exTTF causes a dramatic decrease in the fluorescence intensity of **4** (in toluene, the quantum yield is only 0.0013). It is

Table 2. ^{19}F NMR data.[a]

compound **1**[b]										
δ [ppm]	−59.2	−61.5	−62.1	−62.2	−62.4	−62.8	−63.4	−64.3	−67.6[c]	−70.7[c]
J_{FF} [Hz]	11, 16	13–14	14–15	15–16	13–14	13–14	11, 16	10, 14	15.9	10.3
compound **1**										
δ [ppm]	−59.1	−61.5	−62.2	−62.3	−62.5	−62.8	−63.5	−64.3	−67.6[c]	−70.7[c]
J_{FF} [Hz]	10.0–10.5	12.7–13.2	14.5–14.9	15.0–15.8	13.6–13.9	13.4–14.4	10.5–10.9	10.5–12.7	15.3	10.1
compound **4**										
δ [ppm]	−59.9	−61.6	−61.9	−62.5	−62.9	−63.0	−63.4	−64.4	−67.9[c]	−70.7[c]
J_{FF} [Hz]	8.0–15.7	12.4–13.4	13.8–15.1	12.4–13.7	12.0–13.4	11.7–13.4	10.3–14.6	9.8–13.2	15.7	9.8

[a] All data are from this work, unless otherwise noted; [D_6]benzene solutions at 25 °C; C_6F_6 internal standard ($\delta = -164.9$). Coupling constants are known to $\pm$0.2 Hz for terminal CF_3 quartets. Resonances for other CF_3 groups are multiplets; J_{FF} values for the ones that are apparent (but not true) septets are $\pm$1 Hz. [b] Data from reference [14c]. [c] Terminal CF_3 group

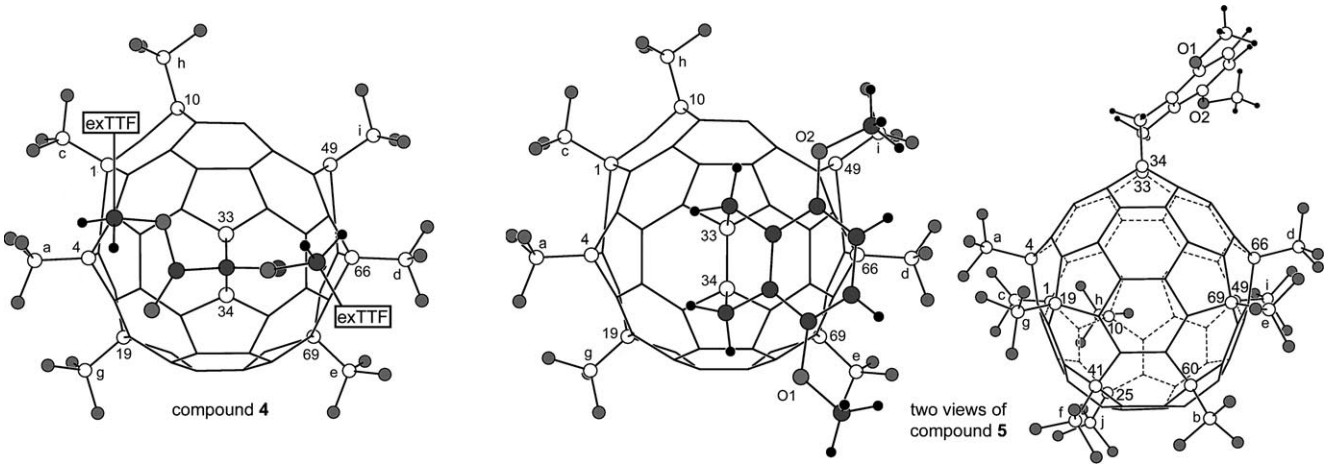

Figure 6. Portion of one possible conformation of structure **4** based on the X-ray structure of **2**[18] (left) and two views of the structure of **5**.[21]

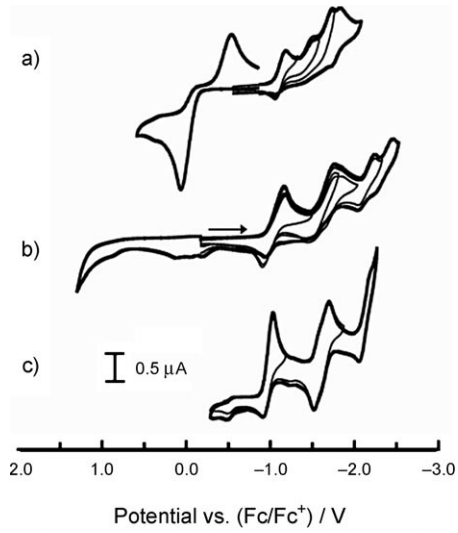

Figure 7. Cyclic voltammograms of a) **4**, b) **2**, and c) **1**.

Table 3. Redox potentials.[a,b]

	E^1_{ox}	E^1_{red}	E^2_{red}	E^3_{red}
1	–	−0.95[c]	−1.53	−2.21[c]
2	–	−1.10	−1.70	−1.82[c]
3	+0.18[d]	−1.46[c]	–	–
4	+0.07[d]	−1.15	−1.44[c]	−1.71[c]
C_{60}[e]	–	−0.90	−1.49	−2.06

[a] Values given in V vs. Fc/Fc^+, obtained by CV and DPV. [b] CV: scan rate, 50 mV s^{-1}. DPV: modulation amplitude, 25 mV; potential step, 5 mV; modulation time, 50 mV; interval time, 500 ms. [c] Irreversible. Cathodic peak potentials. [d] Irreversible two-electron oxidation. Anodic peak potentials. [e] From reference [26].

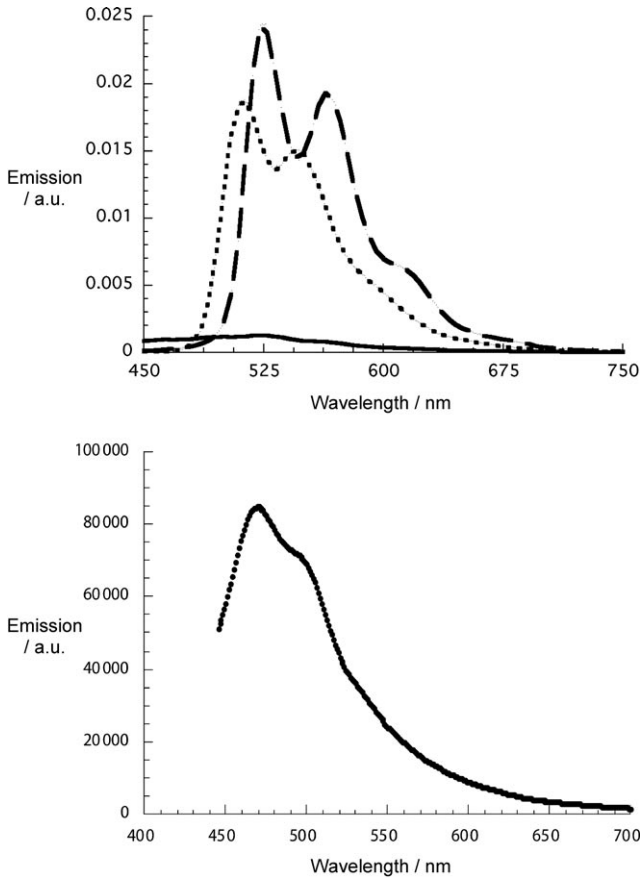

Figure 8. Top: Room-temperature fluorescence spectra of toluene solutions of **1** (dotted line), **2** (dashed line), and **4** (solid line), exhibiting the same optical absorption of 0.05 at the 355 nm excitation wavelength. Bottom: Room-temperature fluorescence spectra of toluene solutions of **3** exhibiting an optical absorption of 0.05 at the 355 nm excitation wavelength.

important that, although the yield drops, the emission patterns of C_1-$C_{70}(CF_3)_{10}$ are not affected by the presence of the electron-donating exTTF. A strongly exothermic electron transfer deactivation is implicit, during which the fullerene 2.36 eV singlet excited state is readily transformed into a 1.22 eV highly energetic radical–ion pair. Complementary experiments, in which the emissive features of exTTF were scrutinized in **3** and **4**, did not disclose any notable differences. The latter finding is rationalized on the basis of the intrinsically short lifetime of exTTF-centered excited states (vide infra).

Upon modifying the solvent polarity from toluene ($\varepsilon=2.38$) to THF ($\varepsilon=7.6$) to benzonitrile ($\varepsilon=24.8$), a gradual intensification of the C_1-$C_{70}(CF_3)_{10}$ fluorescence quenching is discernible for **4**. In THF the quantum yield is, for example, 0.00024. Notably, a better solvation of charged species in the more polar media results in: 1) lower energies of the radical–ion pair states, and 2) larger energy gaps relative to the photoexcited singlet state. Thus, the trend in solvent polarity is attributed to intramolecular charge transfer reactions, which are facilitated by larger driving forces.

An independent probe for the magnitude of electron transfer quenching is fluorescence lifetime experiments. For this we followed the 465 and 525 nm maxima of the exTTF and C_1-$C_{70}(CF_3)_{10}$ fluorescence, respectively, as a function of time. Importantly, fluorescence lifetime experiments allow segregation of the contributions of exTTF from those of C_1-$C_{70}(CF_3)_{10}$. Focusing on the exTTF emission first, neither for **3** nor for **4** were any detectable features seen. Turning to the C_1-$C_{70}(CF_3)_{10}$ fluorescence, the decay curves of the references were best fitted by a single exponential decay. For **2** the lifetimes were 3.4 ns (toluene), 3.1 ns (THF), and 3.5 ns (benzonitrile). For **4**, on the other hand, the fluorescence deactivation falls within the time resolution of our apparatus, which is approximately 0.1 ns. This suggests a rapid electron transfer deactivation of the photoexcited C_1-$C_{70}(CF_3)_{10}$.

In summary, steady-state and time-resolved fluorescence measurements testify that a solvent-dependent and rapid decay of the C_1-$C_{70}(CF_3)_{10}$ singlet excited state prevails in **4**. Conclusive information about the photoproducts came from transient absorption spectroscopy. In particular, with the help of femtosecond laser pulses at 387 nm, the fate of the exTTF and the C_1-$C_{70}(CF_3)_{10}$ singlet excited states was probed. Following the time evolution of the characteristic singlet excited-state features of exTTF and C_1-$C_{70}(CF_3)_{10}$ is a convenient mode to identify spectral features of the resulting photoproducts and to determine absolute rate constants for the intramolecular decay.

The known excited-state properties of exTTF will now be discussed,[27] because they emerge as important reference points for the interpretation of the features expected in **4**. Photoexcitation of **3** at 387 nm generates an exTTF-centered excited state (not shown). Spectral characteristics of this very short-lived excited state (1.2 ps) are transient maxima around 465, 605, and 990 nm, as well as a transient minimum at 440 nm.[28] The short lifetimes (i.e., after 5 ps no transient absorption remains) are rationalized by the presence of the sulfur atoms, with a strong second-order vibronic spin-orbit coupling.[29]

On the other hand, the differential spectra recorded immediately after the laser pulse for C_1-$C_{70}(CF_3)_{10}$ in **1** and **2** are characterized, for example, in the near-infrared by a broad absorption with its maximum at 1050 nm.[30] Such a spectral attribute is, in line with what is known for fullerenes in general,[31] indicative of the C_1-$C_{70}(CF_3)_{10}$ singlet excited state, and is formed with a rate constant of $1\times10^{12}\ s^{-1}$ (see Figure 9). The singlet excited state features decay slowly

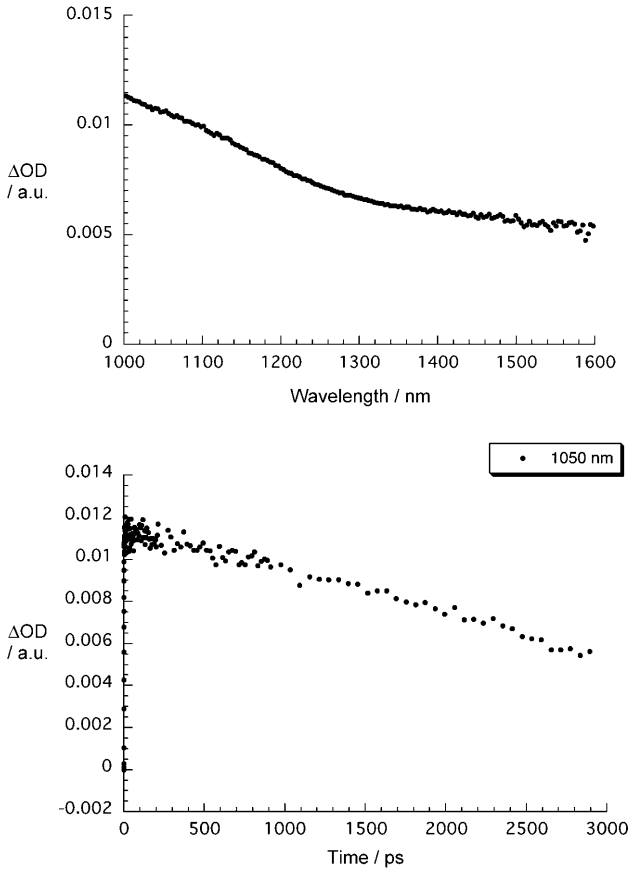

Figure 9. Top: Differential absorption spectra (near-infrared) obtained upon femtosecond flash photolysis (387 nm; 100 nJ) of **2** ($\approx10^{-6}$ M) in argon-saturated toluene at room temperature. Bottom: Time absorption profiles at 1050 nm of the spectra shown above, monitoring the intersystem crossing.

($4.1\times10^{8}\ s^{-1}$) to the energetically lower lying triplet excited state predominantly through intersystem crossing.

Regarding the femtosecond transient absorption measurements of **4**, immediately after the laser excitation, the strong singlet–singlet absorptions of exTTF (i.e., maxima at 465, 605, and 990 nm; minimum at 440 nm)[28] and C_1-$C_{70}(CF_3)_{10}$ (i.e., maximum at 1050 nm)[30] start to grow, (about $1\times10^{12}\ s^{-1}$, Figure 10). This confirms, despite linking both constituents, the successful formation of the exTTF and C_1-$C_{70}(CF_3)_{10}$ singlet excited states. Instead of seeing, however, slow ISC dynamics, as, for example, the C_1-$C_{70}(CF_3)_{10}$ references (**1** and **2**) exhibit, the singlet–singlet absorptions decay in the presence of the electron-donating exTTF with accelerated dynamics. The singlet excited-state lifetimes, as they were determined from an average of first-order fits of the time-absorption profiles at various wavelengths, are very short (i.e., in the order of 2 ps); an example is given in Figure 10. The singlet lifetimes can be employed using Equation (1) to determine the electron transfer rates of about $5.0\times10^{11}\ s^{-1}$.

$$k=1/\tau_{(dyad)}-1/\tau_{(reference)} \quad (1)$$

Spectroscopically, the transient absorption changes, taken after the completion of the decay, bear no resemblance to any of the aforementioned excited states of exTTF or C_1-$C_{70}(CF_3)_{10}$. In particular, in toluene the new transient is ascribed to a product that evolves from an intramolecular electron-transfer reaction. Spectroscopic proof for the radical–ion pair formation was obtained from the features developing in parallel with the disappearance of the exTTF and C_1-$C_{70}(CF_3)_{10}$ singlet–singlet absorption, which are exemplified in Figures 10 and 11. In the visible region, a set of two maxima at 610 and 660 nm corresponds to the one-electron oxidized exTTF$^{\bullet+}$,[28] whereas in the near-infrared region the 1450 nm maximum resembles the signature of the one-electron reduced C_1-$C_{70}(CF_3)_{10}^{\bullet-}$.[32] In THF and benzonitrile, the

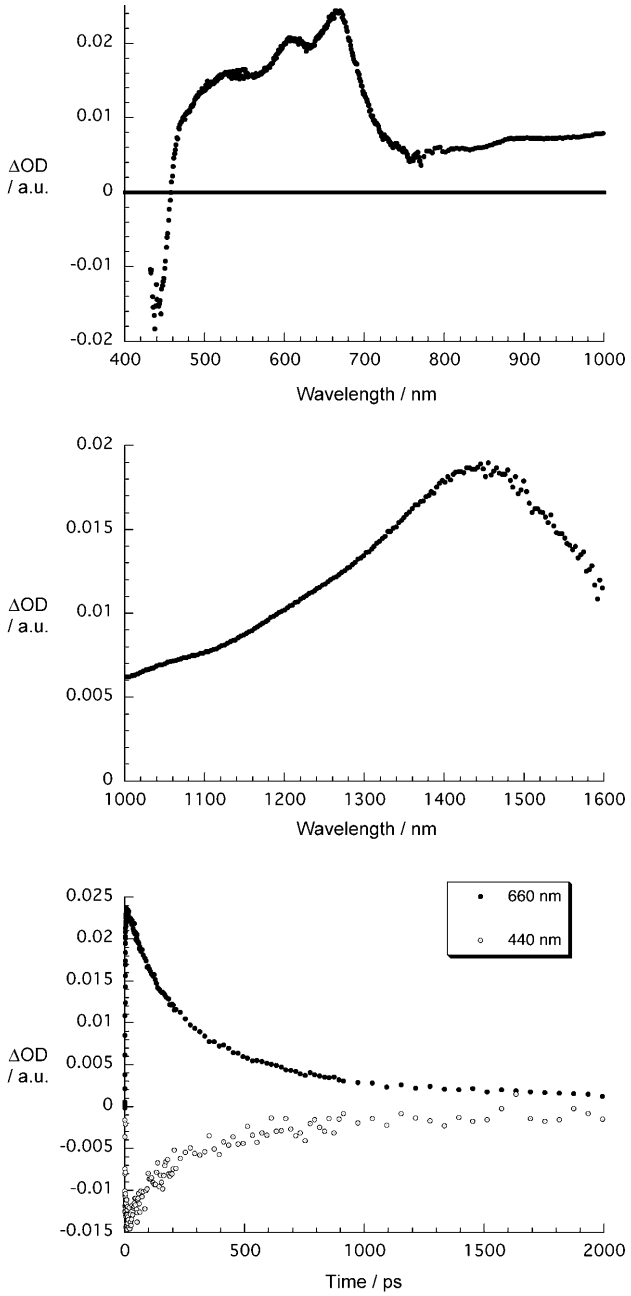

Figure 10. Upper part: Differential absorption spectra (visible and near-infrared) obtained upon femtosecond flash photolysis (387 nm) of **4** ($\approx 10^{-6}$ M) in argon-saturated toluene at room temperature. Central part: Differential absorption spectra (extended near-infrared) obtained upon femtosecond flash photolysis (387 nm) of **4** ($\approx 10^{-6}$ M) in argon-saturated toluene at room temperature. Lower part: Time absorption profiles at 440 and 660 nm for the spectra shown above, monitoring the charge separation and charge recombination in toluene.

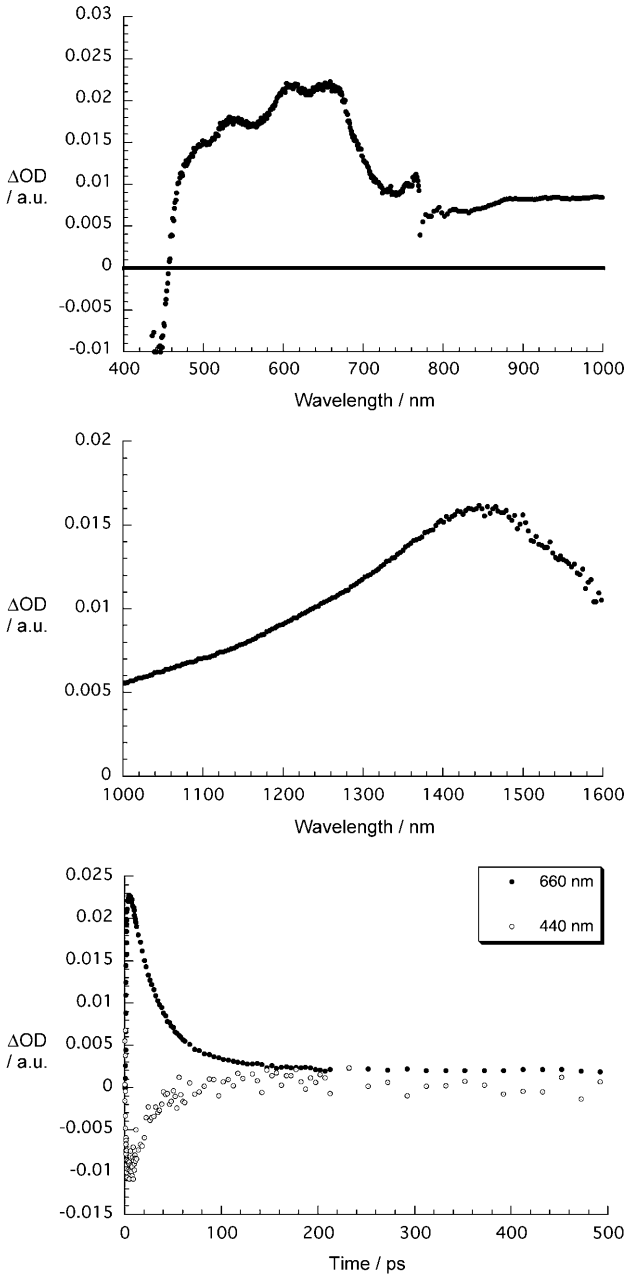

Figure 11. Upper part: Differential absorption spectra (visible and near-infrared) obtained upon femtosecond flash photolysis (387 nm) of **4** ($\approx 10^{-6}$ M) in argon-saturated benzonitrile at room temperature. Central part: Differential absorption spectra (extended near-infrared) obtained upon femtosecond flash photolysis (387 nm) of **4** ($\approx 10^{-6}$ M) in argon-saturated benzonitrile at room temperature. Lower part: Time absorption profiles at 440 and 660 nm for the spectra shown above, monitoring the charge separation and charge recombination in benzonitrile.

same radical–ion pair state features were seen to be formed. All radical–ion pair attributes (see Figures 10 and 11) decay on the picosecond timescale. It is important that the decay of both probes resemble one another, and give rise to kinetics that obey a clean unimolecular rate law. The rates range from 289 to 23 ps in toluene and benzonitrile, respectively. In line with such a fast charge recombination, differential absorption changes, recorded immediately after an 8 ns pulse, failed to generate any spectral features at all.

Conclusion

In the current work we have improved the yield and efficiency for the synthesis of the perfluoroalkylfullerene **1** by using Cu powder in the heated-flow-tube method previously reported by some of us.[16] The new protocol gives access to hundreds of milligrams of this higher fullerene species, and thus widens the synthetic capability in the design and preparation of new fullerene derivatives In particular, it has allowed the preparation of the first exTTF$_2$–$C_{70}(CF_3)_{10}$ dyad in satisfactory yields. The high purity of the Bingel adduct obtained (**4**) has enabled the detailed characterization of the NMR features of the functionalized fullerene cage, as well as the exTTF backbones by 1D (^{1}H, ^{13}C, and ^{19}F) and 2D (HMQC and HMBC) NMR studies.

The electronic properties of this new fullerene derivative have been probed by UV/Vis spectroscopic analysis, which suggests only weak interactions between the redox chromophores in their ground state. This is further supported by electrochemical studies using the CV method. Fluorescence and time-resolved and steady-state experiments in different solvents were carried out to determine the photophysical behavior of the new compound. The perfluoroalkylfullerene singlet excited state deactivated through an intramolecular electron transfer process, affording the charged-separated radical pair, which decays rather rapidly with rates from 289 to 23 ps in toluene and benzonitrile, respectively. The charged-separated radical pair was unequivocally confirmed by the spectral fingerprints of C_1-$C_{70}(CF_3)_{10}^{\bullet-}$ (1450 nm) and exTTF$^{\bullet+}$ (660 nm).

Experimental Section

General: All solvents were dried according to standard procedures. Reagents were used as purchased, unless otherwise specified. Flash chromatography was performed using silica gel (Merck, Kieselgel 60, 230–240 mesh or Scharlau 60, 230–240 mesh). Analytical thin-layer chromatography (TLC) was performed using aluminum-coated Merck Kieselgel 60 F254 plates. High-performance liquid chromatography (HPLC) was performed on an Agilent 1100 LC. HPLC grade solvents were used as the eluents. Injection volumes of samples were 25 μL for analyses, and 1.5 mL for preparations. The ^{1}H and ^{13}C NMR measurements were carried out on a Bruker AVANCE 300 spectrometer or a Bruker AVANCE 500 spectrometer with a CryoProbe system, and TMS was used as an internal reference ($\delta = 0.00$ ppm). The ^{19}F NMR measurements were performed on a Bruker AVANCE 300 spectrometer, with C_6F_6 used as internal reference ($\delta = -164.9$ ppm). Coupling constants (J) are given in Hz and chemical shifts in ppm. Multiplicities are denoted as follows: s = singlet, d = doublet, t = triplet, m = multiplet, br = broad. Absorption spectra were recorded in a Varian Cary 50 spectrophotometer. Matrix-assisted laser-desorption-ionization (coupled to a time-of-flight analyzer) experiments (MALDI-TOF) were recorded on a Bruker REFLEX spectrometer. Cyclic voltammetry (CV) and differential pulse voltammetry (DPV) were performed using an Autolab PGStat 30 instrument. A glassy carbon working electrode (Metrohm 6.0804.010) was used after being polished with alumina (0.3 μm) for 1 min, and a platinum wire was used as the counter electrode. An Ag/$AgNO_3$ electrode was used as reference, and potentials are reported vs. the ferrocene/ferrocinium couple used as internal reference. The solvent/electrolyte used was anhydrous THF containing 0.1 M tetrabutylammonium hexafluorophosphate ($TBAPF_6$). The solution was deaerated by bubbling with argon for 20 min prior to the electrochemical measurements. Femtosecond transient absorption studies were performed with 387 nm laser pulses (1 kHz, 150 fs pulse width) from an amplified Ti:Sapphire laser system (Model CPA 2101, Clark-MXR Inc.). Compounds **2**[17] and **3**[19] were prepared according to previously reported synthetic procedures, and showed identical spectroscopic properties to those reported in the cited publications.

Synthesis and isolation of C_1-$C_{70}(CF_3)_{10}$ (1): Trifluoromethylation reactions were carried out in the glass tube as follows. Finely ground powder of C_{70} was mixed thoroughly with the Cu powder and loaded in the glass tube. The reactor was first filled with argon gas and heated to the desired temperature, and then argon was replaced with the flow of CF_3I gas (0.2 L h^{-1}). The sublimed product was deposited on the cold end of the tube as brown powder. Due to the presence of the Cu powder, iodine that formed upon decomposition of CF_3I was converted into CuI. Crude products from experiments 1, 3, and 4 (Table 1, total of 659 mg) were dissolved in heptane, filtered, and subjected to a two-stage HPLC procedure using Buckyprep HPLC column (250 × 20 mm i.d., Nacalai Tescue Co., Japan). The first stage involved use of toluene as the eluent and isolation of the fraction containing the main product C_1-$C_{70}(CF_3)_{10}$, eluting at 3.8 min (flow rate 16 mL min^{-1}). In the second stage, 20% toluene: 80% heptane was used as eluent, and purification of the C_1-$C_{70}(CF_3)_{10}$ compound to 98% (HPLC data) was achieved; 483 mg of pure C_1-$C_{70}(CF_3)_{10}$ was thus isolated.

Synthesis of C_1-$C_{70}(CF_3)_{10}$(C(COOEt)$_2$) (2):[17] DBU (12.2 mg, 8.01×10^{-5} mol) was added to a solution of **1** (19.5 mg, 1.27×10^{-5} mol), CBr_4 (7.40 mg, 2.23×10^{-5} mol), and diethyl malonate (3.40 mg, 2.12×10^{-5} mol) in toluene (20 mL), and the solution was stirred at room temperature under an argon atmosphere. The reaction was monitored by TLC and HPLC. After 2 h, the reaction mixture was washed three times with H_2O (10 mL). The organic layer was dried with Na_2SO_4, and the solvent was removed under reduced pressure. The residue was purified by flash column chromatography (SiO_2, 25% hexane in CH_2Cl_2). Further purification was accomplished by one-step HPLC separation (Buckyprep column, ϕ10 × 250 mm). Compound **2** (9.4 g, 6.1×10^{-6} mol, 48%) was obtained as an orange solid. ^{1}H NMR (300 MHz, $CDCl_3$, 298 K): $\delta = 4.42$ (q, $J = 7.08$ Hz, 4H; CH_2), 1.35 ppm (t, $J = 7.08$ Hz, 6H; CH_3,); UV/Vis ($CHCl_3$): $\lambda_{max} = 389$, 442, 471, 505 nm; MALDI-TOF MS: m/z calcd for $C_{87}H_{10}F_{30}O_4$ $[M]^+$: 1688.01; found: 1688.03.

Synthesis of C_1-$C_{70}(CF_3)_{10}$(C(COOCH$_2$exTTF)$_2$) (4): DBU (6.06 mg, 3.98×10^{-5} mol) was added to a solution of **1** (20.0 mg, 1.31×10^{-5} mol), CBr_4 (6.64 mg, 2.00×10^{-5} mol), and **3**[19] (15.74 mg, 3.00×10^{-5} mol) in toluene (13 mL), and the resulting solution was protected from light and stirred at room temperature under an argon atmosphere. The reaction was monitored by TLC and HPLC. After 2 h, 6 mg of the starting fullerene was consumed, the reaction mixture was washed three times with H_2O (10 mL). The organic layer was dried with Na_2SO_4, and the solvent was removed under reduced pressure. The residue was purified by flash column chromatography, (SiO_2, 25/75 hexane/CH_2Cl_2). Further purification was accomplished by one-step HPLC separation (10 × 250 mm Buckyprep column). Compound **4** was obtained as a brownish orange solid in 80% yield (based on consumed fullerene material). ^{1}H NMR (300 MHz, [D$_8$]THF, 298 K): $\delta = 7.82$–7.54 (m, 7H; CH), 7.37–6.97 (m, 7H; CH), 6.57–6.29 (m, 8H; SCH), 5.61–5.19 ppm (m, 4H; CH_2); ^{13}C NMR (125 MHz, [D$_8$]THF, 283 K): $\delta = 162.1$ (*C*OO), 162.0 (*C*OO), 156.1, 153.7,

153.5, 152.9, 152.3, 151.5, 151.3, 151.2, 150.2, 150.0, 149.9, 149.7, 149.3, 149.2 (2C), 149.1, 147.9 (2C), 147.3, 147.2 (2C), 146.7, 146.5, 146.2, 146.1, 145.7, 145.6, 144.9, 144.8, 144.7, 143.9, 143.8, 143.7, 143.6, 141.7, 141.6, 141.5, 141.4, 141.2, 141.1 (2C), 141.0, 140.8, 140.1, 139.7, 137.0, 136.8 (SCS), 136.6 (SCS, 2C), 136.4 (SCS), 135.3 (CCCH, 2C), 135.3, 135.2 (2C; CCCH), 134.9 (CCCH), 134.8 (2C; CCCH), 134.7 (CCCH), 133.8 (2C), 131.7 ($(CH)_2CCH_2$), 131.6, 131.3 ($(CH)_2CCH_2$), 131.3, 129.4, 129.0, 128.9, 128.2, 128.1, 127.4, 126.9, 125.3 (2C; CH), 125.2 (2C; CH), 124.7 (CH), 124.7 (2C; CH), 124.4 (2C; CH), 124.3 (2C; CH), 124.2 (CH), 122.8 (q, J_{C-F}=282.5 Hz, 3C; CF_3), 122.7 (q, J_{C-F}=280.0 Hz, 2C; CF_3), 122.6 (q, J_{C-F}=281.3 Hz, 2C; CF_3), 122.5 (q, J_{C-F}=281.3 Hz, 1C; CF_3,), 122.4 (q, J_{C-F}=281.3 Hz, 1C; CF_3), 122.2 (q, J_{C-F}=280.0 Hz, 1C; CF_3,), 120.6 (2C; CCCC), 120.5 (CCCC), 120.4 (CCCC), 117.0 (SCH), 116.9 (2C; SCH), 116.8 (3C; SCH), 116.7 (2C; SCH), 70.9 (sp^3 carbon on the cage), 69.1 (sp^3 carbon on the cage), 68.4 (CH_2), 68.3 (CH_2), 62.3 (q, $^2J_{C-F}$=32.3 Hz, 2C; C-CF_3), 61.6 (q, $^2J_{C-F}$=32.1 Hz, 1C; C-CF_3), 61.1 (q, $^2J_{C-F}$=33.9 Hz, 1C; C-CF_3), 60.9 (q, $^2J_{C-F}$=33.5 Hz, 1C; C-CF_3), 60.8 (q, $^2J_{C-F}$=33.5 Hz, 1C; C-CF_3), 60.6 (q, $^2J_{C-F}$=33.9 Hz, 1C; C-CF_3), 59.9 (q, $^2J_{C-F}$=34.5 Hz, 1C; C-CF_3), 59.6 (q, $^2J_{C-F}$=33.1 Hz, 1C; C-CF_3), 57.3 (q, $^2J_{C-F}$=33.5 Hz, 1C; C-CF_3), 43.9 ppm (COOCCOO); UV/Vis ($CHCl_3$) λ_{max}=368, 436 nm; MALDI-TOF MS: *m/z* calcd for $C_{123}H_{26}F_{30}O_4S_8$ $[M]^+$: 2416.92; found: 2416.95.

Acknowledgements

Financial support from the Deutsche Forschungsgemeinschaft (SFB 583), the Volkswagen Foundation (I-77/855), the Office of Basic Energy Sciences of the U.S. Department of Energy, the U.S. National Science Foundation (CHE-0707223), Grant-in-Aid for Scientific Research on Innovative Areas (20108001, "π-Space"), a Grant-in-Aid for Scientific Research (A) (20245006), the 21st Century COE Program, the Next Generation Super Computing Project (Nanoscience Project), the Nanotechnology Support Project, Grants-in Aid for Scientific Research on Priority Areas (20036008, 20038007) from the Ministry of Education, Culture, Sports, Science, and Technology of Japan, the MEC of Spain (projects CTQ2008-00795 and Consolider-Ingenio 2010 CSD2007-0010, Nanociencia Molecular) and the CAM (project P-PPQ-000225-0505) is greatly appreciated.

[1] a) M. R. Wasielewski, *Chem. Rev.* **1992**, *92*, 435–461; b) H. Kurreck, M. Huber, *Angew. Chem.* **1995**, *107*, 929–947; *Angew. Chem. Int. Ed. Engl.* **1995**, *34*, 849–866; c) D. Gust, T. A. Moore, A. L. Moore, *Acc. Chem. Res.* **2001**, *34*, 40–48; d) M. R. Wasielewski, *J. Org. Chem.* **2006**, *71*, 5051–5066.

[2] a) C. J. Brabec, N. S. Sariciftci, J. C. Hummelen, *Adv. Funct. Mater.* **2001**, *11*, 15–26; b) C. Winder, N. S. Sariciftci, *J. Mater. Chem.* **2004**, *14*, 1077–1086; c) S. Günes, H. Neugebauer, N. S. Sariciftci, *Chem. Rev.* **2007**, *107*, 1324–1338; d) B. C. Thompson, J. M. J. Fréchet, *Angew. Chem.* **2008**, *120*, 62–82; *Angew. Chem. Int. Ed.* **2008**, *47*, 58–77.

[3] For some books on fullerenes: a) *Fullerenes: From Synthesis to Optoelectronic Properties* (Eds.: D. M. Guldi, N. Martín), Kluver Academic, Dordrecht, **2002**; b) A. Hirsch, *The Chemistry of Fullerenes*, Wiley-VCH, Weinheim, **2005**; c) *Fullerenes. Principles and Applications* (Eds.: F. Langa, J. F. Nierengarten), RSC, Cambridge, **2007**.

[4] For reviews on C_{60}-donor composites, see: a) N. Martín, L. Sánchez, B. M. Illescas, I. Pérez, *Chem. Rev.* **1998**, *98*, 2527–2548; b) D. M. Guldi, *Chem. Commun.* **2000**, 321–327; c) D. M. Guldi, *Chem. Soc. Rev.* **2002**, *31*, 22–36; d) H. Imahori, *J. Phys. Chem. B* **2004**, *108*, 6130–6143; e) J. L. Segura, N. Martín, D. M. Guldi, *Chem. Soc. Rev.* **2005**, *34*, 31–47; f) N. Martín, *Chem. Commun.* **2006**, 2093–2104; g) D. M. Guldi, A. G. M. Rahman, V. Sgobba, C. Ehli, *Chem. Soc. Rev.* **2006**, *35*, 471–487; h) P. V. Kamat, *J. Phys. Chem. C* **2007**, *111*, 2834–2860.

[5] For reviews on exTTFs chemistry and properties, see: a) M. R. Bryce, *J. Mater. Chem.* **2000**, *10*, 589–598; b) J. L. Segura, N. Martín, *Angew. Chem.* **2001**, *113*, 1416–1455; *Angew. Chem. Int. Ed.* **2001**, *40*, 1372–1409; c) M. Bendikov, F. Wudl, D. F. Perepichka, *Chem. Rev.* **2004**, *104*, 4891–4945; d) E. M. Pérez, N. Martín, *Chem. Soc. Rev.* **2008**, *37*, 1512–1519; e) E. M. Pérez, B. M. Illescas, M. A. Herranz, N. Martín, *New J. Chem.* **2009**, *33*, 228–234.

[6] N. Martín, L. Sánchez, M. A. Herranz, B. Illescas, D. M. Guldi, *Acc. Chem. Res.* **2007**, *40*, 1015–1024.

[7] For a recent review, see: J. L. Delgado, M. A. Herranz, N. Martín, *J. Mater. Chem.* **2008**, *18*, 1417–1426.

[8] O. V. Boltalina, S. H. Strauss in *Encyclopedia of Nanoscience and Nanotechnology* (Eds.; J. A. Schwarz, C. Contescu, K. Putyera), Marcel Dekker, New York, **2004**, pp. 1175–1190.

[9] a) O. V. Boltalina, *J. Fluorine Chem.* **2000**, *101*, 273–278; b) O. V. Boltalina, N. A. Galeva, *Russ. Chem. Rev.* **2000**, *69*, 609–621.

[10] a) O. V. Boltalina, A. Y. Borschevskii, L. N. Sidorov, J. M. Street, R. Taylor, *Chem. Commun.* **1996**, 529–530; b) A. A. Gakh, A. A. Tuinman, J. L. Adcock, R. A. Sachleben, R. N. Compton, *J. Am. Chem. Soc.* **1994**, *116*, 819–820; c) V. F. Bagryantsev, A. S. Zapol'skii, O. V. Boltalina, N. A. Galeva, L. N. Sidorov, *Dokl. Chem.* **1997**, *357*, 487–489.

[11] a) O. V. Boltalina, V. Y. Markov, R. Taylor, M. P. Waugh, *Chem. Commun.* **1996**, 2549–2550; b) I. V. Goldt, O. V. Boltalina, L. N. Sidorov, E. Kemnitz, S. I. Troyanov, *Solid State Sci.* **2002**, *4*, 1395–1401.

[12] a) O. V. Boltalina, J. M. Street, R. Taylor, *Chem. Commun.* **1998**, 1827–1828; b) G. A. Burley, A. G. Avent, O. V. Boltalina, T. Drewello, I. V. Goldt, M. Marcaccio, F. Paolucci, D. Paolucci, J. M. Street, R. Taylor, *Org. Biomol. Chem.* **2003**, *1*, 2015–2023.

[13] G. A. Burley, A. G. Avent, O. V. Boltalina, I. V. Goldt, D. M. Guldi, M. Marcaccio, F. Paolucci, D. Paolucci, R. Taylor, *Chem. Commun.* **2003**, 148–149.

[14] a) I. S. Uzkikh, E. I. Dorozhkin, O. V. Boltalina, A. I. Botalin, *Dokl. Akad. Nauk* **2001**, *379*, 344–347; b) A. A. Goryunkov, I. V. Kuvychko, I. N. Ioffe, D. L. Dick, L. N. Sidorov, S. H. Strauss, O. V. Boltalina, *J. Fluorine Chem.* **2003**, *124*, 61–64; c) I. E. Kareev, I. V. Kuvychko, S. F. Lebedkin, S. M. Miller, O. P. Anderson, K. Seppelt, S. H. Strauss, O. V. Boltalina, *J. Am. Chem. Soc.* **2005**, *127*, 8362–8375.

[15] a) A. A. Popov, I. E. Kareev, N. B. Shustova, E. B. Stukalin, S. F. Lebedkin, K. Seppelt, S. H. Strauss, O. V. Boltalina, L. Dunsch, *J. Am. Chem. Soc.* **2007**, *129*, 11551–11568; b) A. A. Popov, I. E. Kareev, N. B. Shustova, S. E. Lebedkin S. H. Strauss, O. V. Boltalina, L. Dunsch, *Chem. Eur. J.* **2008**, *14*, 107–121.

[16] I. E. Kareev, I. V. Kuvychko, A. A. Popov, S. F. Lebedkin, S. M. Miller, O. P. Anderson, S. H. Strauss, O. V. Boltalina, *Angew. Chem.* **2005**, *117*, 8198–8201; *Angew. Chem. Int. Ed.* **2005**, *44*, 7984–7987.

[17] N. Ovchinnikova, D. V. Ignat'eva, N. B. Tamm, S. M. Avdoshenko, A. A. Goryunkov, I. N. Ioffe, V. Y. Markov, S. I. Troyanov, L. N. Sidorov, M. A. Yurovskaya, E. Kemnitz, *New. J. Chem.* **2008**, *32*, 89–93.

[18] a) C. Bingel, *Chem. Ber.* **1993**, *126*, 1957–1959; b) A. Hirsch, I. Lamparth, H. R. Karfunkel, *Angew. Chem.* **1994**, *106*, 453–455; *Angew. Chem. Int. Ed. Engl.* **1994**, *33*, 437–438.

[19] S. González, N. Martín, D. M. Guldi, *J. Org. Chem.* **2003**, *68*, 779–791.

[20] T. Tuttle, J. Gräfenstein, D. Cremer, *Chem. Phys. Lett.* **2004**, *394*, 5–13.

[21] Y. Takano, M. A. Herranz, I. E. Kareev, S. H. Strauss, O. V. Boltalina, T. Akasaka, N. Martín, *J. Org. Chem.* **2009**, *74*, 6902–6905.

[22] L. Echegoyen, L. E. Echegoyen, *Acc. Chem. Res.* **1998**, *31*, 593–601.

[23] J. P. Bourgeois, L. Echegoyen, M. Fibbioli, E. Prestch, F. Diederich, *Angew. Chem.* **1998**, *110*, 2203–2207; *Angew. Chem. Int. Ed.* **1998**, *37*, 2118–2121.

[24] M. A. Herranz, F. Diederich, L. Echegoyen, *Eur. J. Org. Chem.* **2004**, 2299–2316.

[25] M. R. Bryce, A. J. Moore, *J. Chem. Soc. Perkin Trans. 1* **1991**, 157–168.

[26] D. Dubois, G. Moninot, W. Kutner, M. T. Jones, K. M. Kadish, *J. Phys. Chem.* **1992**, *96*, 7137–7145.

[27] M. C. Díaz, M. A. Herranz, B. M. Illescas, N. Martín, N. Godbert, M. Bryce, C. Luo, A. Swartz, G. Anderson, D. M. Guldi, *J. Org. Chem.* **2003**, *68*, 7711–7721.
[28] D. M. Guldi, L. Sánchez, N. Martín, *J. Phys. Chem. B* **2001**, *105*, 7139–7144.
[29] G. Kodis, P. A. Liddell, L. de La Garza, A. L. Moore, A. L. Moore, D. Gust, *J. Mater. Chem.* **2002**, *12*, 2100–2108.
[30] J. W. Arbogast, C. S. Foote, *J. Am. Chem. Soc.* **1991**, *113*, 8886–8889.
[31] D. M. Guldi, M. Prato, *Acc. Chem. Res.* **2000**, *33*, 695–703.
[32] a) R. Del Lawson, D. L. Feldheim, C. A. Foss, P. K. Dorhout, C. M. Elliott, C. R. Martin, B. Parkinson, *J. Phys. Chem.* **1992**, *96*, 7175–7177; b) T. Nojiri, M. M. Alam, H. Konami, A. Wanatabe, M. Ito, *J. Phys. Chem. A* **1997**, *101*, 7943–7947; c) M. Fujitsuka, K. Wanatabe, O. Ito, K. Yamamoto, H. Funasaka, *J. Phys. Chem. A* **1997**, *101*, 7960–7964.

Received: August 24, 2009
Revised: January 4, 2010
Published online: March 5, 2010

